Behavior and Strength of Composite Columns under the Impact of Uniaxial Compression Loading

Anas Nahidh Hassooni
Civil Engineering Department
College of Engineering
University of Baghdad and
Uruk University
Baghdad, Iraq
anasnahidh@gmail.com

Salah R. Al Zaidee
Civil Engineering Department
College of Engineering
University of Baghdad
Baghdad, Iraq
Salahalzaidee2004@googlemail.com

Received: 12 January 2022 | Revised: 3 February 2022 | Accepted: 10 February 2022

Abstract-The Concrete Filled Steel Tube Column (CFST) is classified as a composite structural element. This type of column was adopted as the main loaded member in many buildings due to its excellent mechanical properties. CFST columns have high strength and ductility behavior, and they can sustain heavy loads with high performance. These led to their adoption in many countries. In the current study, the behavior and strength of CFST columns under the effect of axial compression load with parameters such as the diameter to thickness ratio and the height to diameter ratio were investigated. Strength carrying capacity and axial and lateral deformations with axial and lateral strains were explored. The test results showed that smaller heights within the same material gave higher strength capacity. The stiffness of the CFST is more than concrete and hollow steel section specimens' due to its capability of high strength capacity with low displacement. Also, the composite action of CFST gave more stiffness.

Keywords-composite column; CFST; compression load; strength column capacity; column deformation

I. INTRODUCTION

Concrete Filled Steel Tube Columns (CFSTCs) are classified as main structural elements that can carry different types of loading when used as structural members in buildings. This type of structural element has high stability and stiffness due to its superior mechanical properties due to the composite action [1]. Concrete column jacketing is done by steel tubes or Fiber Reinforced Polymer (FRP) sheets with the fibers oriented around the concrete column in order to work like stirrups so that they provide confinement to prevent the formation of plastic hinges, splitting, and buckling [2]. The main purpose of concrete column condiment by steel tubes is to form a composite structural member. The benefits of confinement of a concrete column by steel tubes are increased stiffness, stability, increased strength capacity, and reduced buckling. The presence of steel tubes increases the concrete compressive strength and the column becomes more resistant, not only against gravity loads, but also against lateral loads such as wind or seismic. Authors in [3] studied the influence of confinement by rings around the steel tubes of CFST columns subjected to axial load. The main objective of the proposed methodology is to restrict the elastic lateral dilation of concrete casted inside the steel tube. The test results showed that the suggested ring configuration enhanced the axial load-capacity of CFST columns, improved stiffness, and decreased the strength degradation rate. The presence of steel rings reduced the lateral deformation of CFST columns. Authors in [4] reviewed the applications and development of CFST members. It was shown that this structural member type enhanced stiffness, increased strength, and improved ductility due to the composite action between concrete and steel. Authors in [5] studied the performance of CFST columns under the effect of axial load. Variables like steel tube thickness and reinforcing bars and columns with and without foundations were considered. The experimental tests showed that the presence of reinforcing bars made the composite columns stronger. Bending failure occurred when the weld strength of the casing was greater than the limit of the axial compression load, whereas when the weld strength was less than the limit of the applied load, the failure became open splitting of the steel casing. Authors in [6] studied the mechanism of CFST failure with circular and square cross sections. The full scale of CFST columns under the effect of uniaxial compression load was considered. Finite element analysis was utilized to check out the test results. It was found that the contact pressure at the interface between the concrete core and the surrounding steel tube was uniform. As was pointed out in the experimental tests, the failure mode of the CFST column circular cross section was drum but local buckling occurred in the case of square CFST column. The simulation results showed that the confinement of the steel tube that surrounded the concrete core affected the ultimate load carrying capacity and the ductility of square and circle CFST columns. Authors in [7] studied the effects of steel rings around the external steel tube of the CFST column. The larger Poisson's ratio of steel led to the delamination at the interface between the concrete core and the surrounding steel tube. Theoretical models that predicate and estimate the load-strain as lateral and longitudinal curves were simulated and experimentally tested. The theoretical model results were close to the experimental test results. Authors in [8] studied the

Corresponding author: Anas Nahidh Hassooni

influence of concrete grade of CFST confinement column under axial load. The considered parameters were concrete compressive strength (infill) and diameter/thickness ratio of the steel tube in a total of six specimens. The conducted tests were focused on the strength capacity of the CFST column, stresses in concrete and steel tube, and confinement of column specimens. The test results showed that concrete with low compressive strength had more ductility and confinement. The presence of steel tubes surrounding the concrete core gave passive confinement to the concrete column. Authors in [9] reviewed the stiffening of CFST columns experimentally and theoretically. Authors in [10] studied the performance of CFSTs with high-strength concrete core subjected to axial compression load. Authors in [11] investigated the behavior of CFST columns subjected to axial compression load. Concrete core size, steel tube shape, and diameter/thickness ratio were considered. The experimental tests showed that the most significant parameter affecting the strength capacity of the CFST column was the thickness of steel tube which also had more impact on the degree of confinement of the concrete core. In addition, the load-deformation of circular specimens showed strain-hardening or perfectly plastic behavior after yielding. Authors in [12] proposed a finite element model to predict the performance and strength of CFST columns under the effect of axial load. The predicted behavior of the modified model was verified with experimental data. Authors in [13], studied the behavior of slender columns under the effect of combined loading by simulating the performance of different slender columns under the impact of eccentric axial force. They concluded that concrete strength, level of axial load, and column slender ratio were the most important factors affecting the reduction coefficients and the effective bending stiffness. Authors in [14] estimated the column capacity by testing 9 sandwich column specimens under axial compression load. The columns were made of normal strength concrete, whereas column portions were made from comparatively higher strength concrete. The test results showed that the aspect ratio affects the strength of such columns.

Summarizing the literature review, composite columns have higher strength capacity, stability, and stiffness than reinforced concrete columns or plain steel columns.

II. AIM OF THE CURRENT STUDY

The aim of the present study is to investigate the behavior and strength of concrete-filled steel tubes subjected to uniaxial loading and to compare them with control samples of concrete and steel tube columns. The mechanical properties of the studied concrete and steel tubes, such as compressive, flexural, splitting, and tensile strength and the modulus of elasticity by the stress-strain curve of the tested samples were explored. For the steel section, yielding and stress-strain behavior were studied to obtain the steel modulus of elasticity. The investigation focused into the behavior of the tested specimens and recorded the experimental data that represent column capacity strength, buckling, and longitudinal and lateral displacements. Different specimens were prepared and tested considering different parameters such as slenderness ratio and confinement steel tube sections.

III. EXPERIMENTAL PART

A. Material Preparation

Three columns with different heights (400, 800, and 1200wmm) were designed with steel tube thicknesses of 1.35mm and concrete core diameter of 76mm. The specimens were tested under the effect of uniaxial compression load. The concrete and steel tube's mechanical properties are listed in Table I, in which the concrete mechanical properties are based on [15] for compressive strength, [16] for splitting tensile strength, [17] for modulus of rupture, and [18] for modulus of elasticity. The mechanical steel tube by tensile test was based on [19]. Water - cement ratio for concrete core was 0.38 and the average of 3 specimens for each tested concrete was adopted.

TABLE I. MECHANICAL PROPERTIES

Concrete			Steel tube	
f_c' (MPa)	Ec (MPa)	f_r (MPa)	f_y (MPa)	Es (MPa)
48	41500	7.55	295	205000

TABLE II. MODEL MARKS

Mark	Description	Specimen geometry						
		Concrete core diameter (mm)	Steel tube (mm)					
			Do	t	Di	h ($\times 10^2$)	ht/Do	Do/t
CC	Concrete	73.3	-	-	-	4	5.46	-
						8	10.91	
						12	16.37	
HSC	Steel	-	76	1.35	73.3	4	5.26	56.3
						8	10.53	
						12	15.79	
CFST	Composite	73.3	76	1.35	73.3	4	5.26	56.3
						8	10.53	
						12	15.79	

In Table II, Do is the outer diameter, t is the steel tube thickness, Di is the inner diameter, and h is the specimen height. Figure 1shows the specimens of hollow steel section, concrete and composite respectively, while Figure 2 present the specimen setup under the machine test.

B. Preparation of Specimens

Each hollow steel tube specimen was prepped carefully by cutting the required specimen height (400, 800 or 1200mm) and then making the end smooth and level to ensure that the applied load was distributed symmetrically. Concrete was inserted in the mold after it was oiled to prevent the adhesion between the concrete surface and the inner mold. For CFST specimens, the steel tubes were cleaned from unrequired materials such as dust to ensure there is suitable interaction between them and concrete. The bottoms of the steel tubes were closed with silicone and thick steel plates that were removed before testing the specimen and after the concrete was poured. The top of each specimen (rounded 5mm) was left empty to level the concrete by epoxy. Each specimen was placed at the center of the testing machine to avoid eccentric loading. Then, compressive load was applied at a constant rate. Axial and lateral displacement and strain were recorded for each applied load step up to failure for each column type (HSC, CC, and CFST).

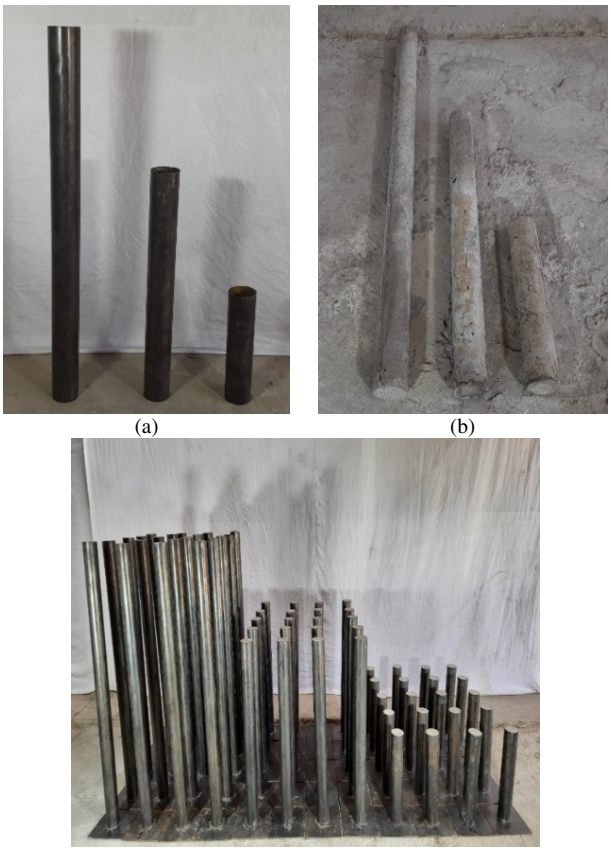

(a) (b)

(c)

Fig. 1. (a) Steel specimens (HSC), (b) concrete specimens (CC), and (c) composite specimens (CFST).

Fig. 2. Specimen setup.

IV. TEST RESULTS

Figures 3-14 show the axial and lateral load-displacement and longitudinal and lateral load-strain for all tested specimens. All tested specimens behaved nonlinearly up to the inflection point that depends on the parameters and specifications of each specimen. This inflection point relies on many parameters such as slenderness ratio, column type, and applied load. Each specimen reached maximum load capacity and after that the applied load dropped down, but they gave displacement at failure greater than the displacement at maximum load.

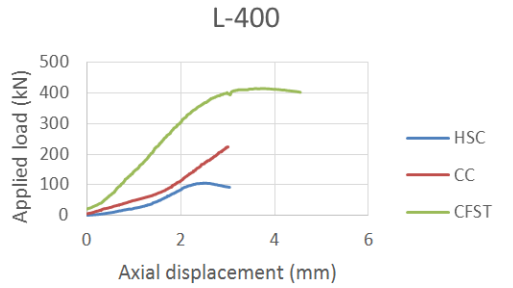

Fig. 3. Applied load-axial displacement variation for h= 400mm.

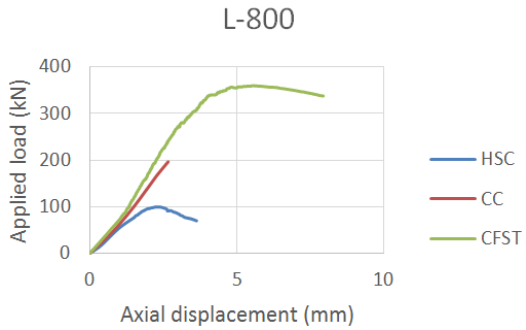

Fig. 4. Applied load-axial displacement variation for h=800mm.

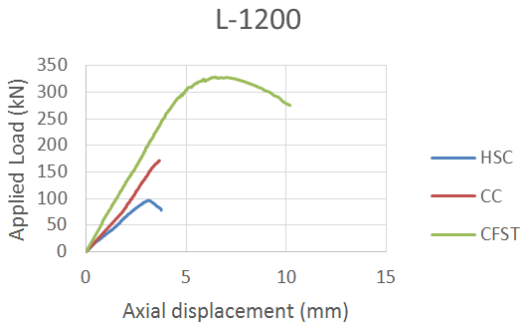

Fig. 5. Applied load-axial displacement variation for h=1200mm.

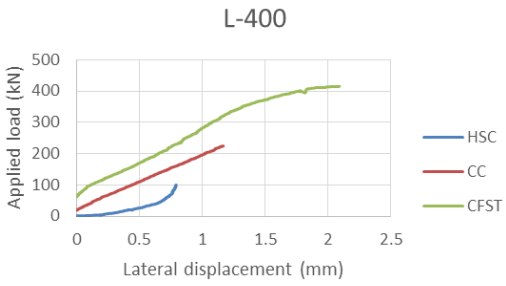

Fig. 6. Applied load-lateral displacement variation for h=400mm.

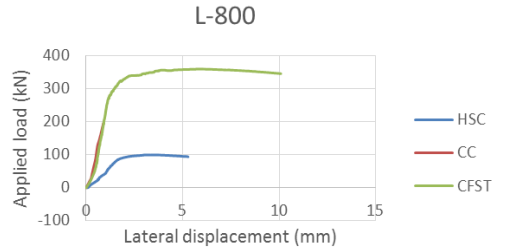

Fig. 7. Applied load-lateral displacement variation for h=800mm.

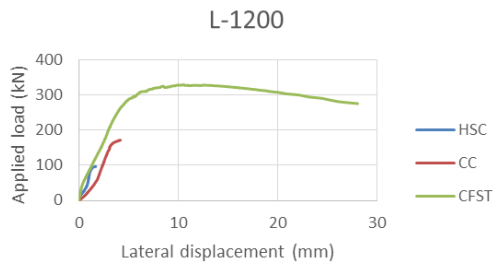

Fig. 8. Applied load-lateral displacement variation for h=1200mm.

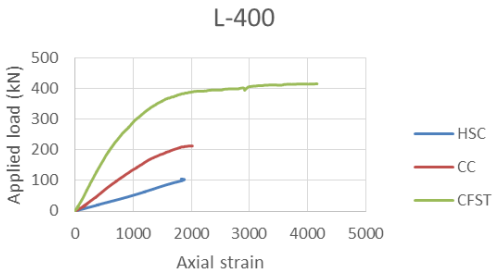

Fig. 9. Applied load-axial strain variation for h=400mm.

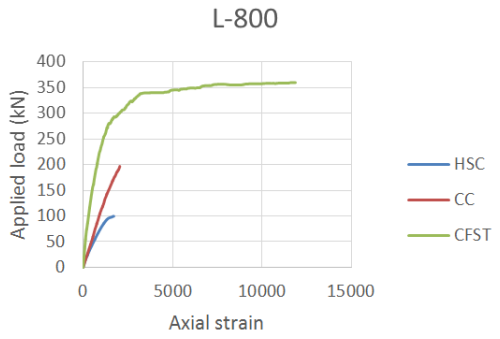

Fig. 10. Applied load-axial strain variation for h=800mm.

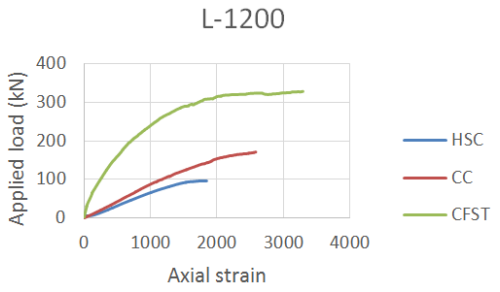

Fig. 11. Applied load-axial strain variation for h=1200mm.

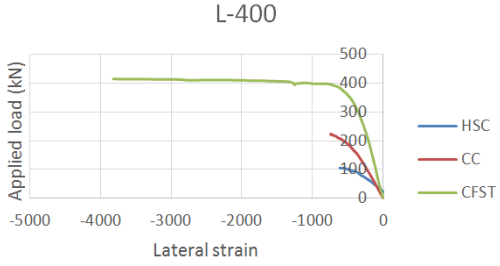

Fig. 12. Applied load-lateral strain variation for h=400mm.

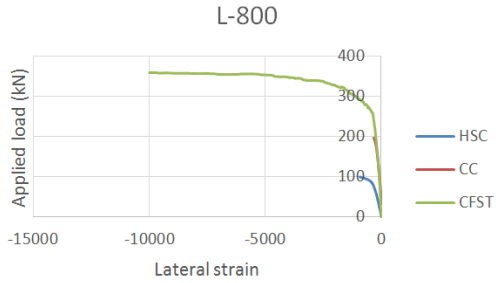

Fig. 13. Applied load-lateral strain variation for h=800mm.

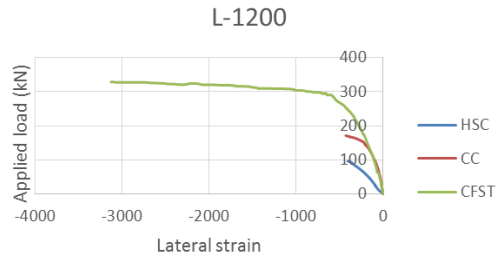

Fig. 14. Applied load-lateral strain variation for h=1200mm.

The ductility of a structural member is the ability to bear or endure considerable deflection before failure. The ductility of a structural element is a very important quality indicator because it provides signs of collapse or failure, so the total collapse of a structural member may be prevented while the member can undergo more deformations (large deformations) without fail. Concrete is a brittle material, so the presence of steel tubes that surrounds the concrete core enhances its properties. The ductility U for all tested specimens is calculated by dividing the deflection at ultimate load Δ_u by the deflection at yield Δ_y:

$$U = \frac{\Delta_u}{\Delta_y} \quad (1)$$

The stiffness of the tested specimens is the resistance of an elastic body to deflection or deformation by an applied force. The stiffness μ is defined as the ratio of the ultimate load P_u to ultimate load deflection Δ_u:

$$\mu = \frac{P_u}{\Delta_u} \quad (2)$$

Figures 15 to 18 show the axial and lateral ductility and stiffness of all tested specimens. Concrete specimens have a constant ductility because concrete is a brittle material so that there is a plastic zone so the displacement at failure is approximately the same with the one at maximum load. The ductility of HSC specimens is more than concrete specimens' with the same height because steel is a ductile material. The CFST specimen with 1200mm height has longitudinal (axial) ductility more than the other specimens. Regarding the lateral displacement, the ductility of concrete was about the same, the HSC specimen with 800mm height had more than the other specimens, and the CFST with 1200mm height was the highest among the CFST specimens.

TABLE III. TEST RESULTS-AXIAL DISPLACEMENT AND STRAIN BASED ON MAXIMUM AND FAILURE LOAD

Mark	Height (mm)	Test results					
		Max. load (kN)	Failure load (kN)	Max. axial displacement (mm)	Axial displacement at failure (mm)	Max. strain	Strain at failure load
CC	400	224.00	225.00	3.00	3.02	2019	2053
	800	196.64	197.00	2.66	2.68	2025	2050
	1200	171.30	171.60	3.65	3.68	2575	2595
HSC	400	104.66	91.78	2.47	3.04	1876	1900
	800	99.40	69.56	2.27	3.63	1672	1700
	1200	96.08	78.04	3.15	3.75	1844	1875
CFST	400	415.08	402.98	3.76	4.55	4159	4300
	800	358.86	338.06	5.59	7.94	11832	11880
	1200	327.81	275.51	6.99	10.19	3296	3330

TABLE IV. TEST RESULTS-LATERAL DISPLACEMENT AND LATERAL STRAIN BASED ON MAXIMUM AND FAILURE LOAD

Mark	Height (mm)	Test results					
		Max. load (kN)	Failure load (kN)	Max. lateral displacement (mm)	Lateral displacement at failure (mm)	Max. strain	Strain at failure load
CC	400	224.00	225.00	1.16	1.17	700	755
	800	196.64	197.00	0.90	0.91	307	365
	1200	171.30	171.60	4.03	4.05	408	470
HSC	400	104.66	91.78	0.8	1.15	585	625
	800	99.40	69.56	4.05	5.28	785	920
	1200	96.08	78.04	1.17	1.22	380	420
CFST	400	415.08	402.98	2.08	2.21	2913	3784
	800	358.86	338.06	8.44	10.08	5936	9986
	1200	327.81	275.51	11.87	28.06	2190	3125

TABLE V. AXIAL AND LATERAL DUCTILITY AND STIFFNESS

Mark	Height (mm)	Ductility (axial)	Stiffness (axial) (kN/mm)	Ductility (lateral)	Stiffness (lateral) (kN/mm)
CC	400	1.01	74.67	1.01	193.10
	800	1.01	73.92	1.01	218.49
	1200	1.01	46.93	1.00	42.51
HSC	400	1.23	42.37	1.44	130.83
	800	1.60	43.79	1.30	24.54
	1200	1.19	30.50	1.04	82.12
CFST	400	1.21	110.39	1.06	199.56
	800	1.42	64.20	1.19	42.52
	1200	1.46	46.90	2.36	27.62

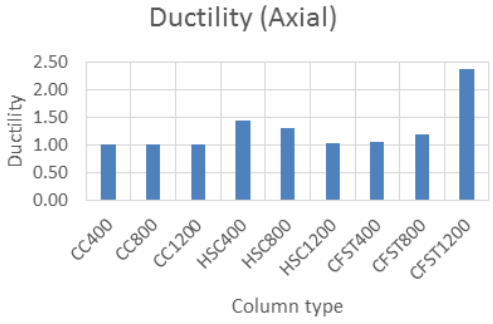

Fig. 15. Axial ductility variation of all specimens.

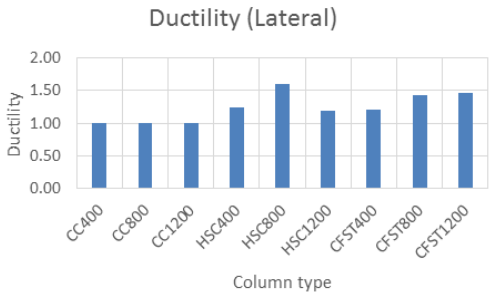

Fig. 16. Lateral ductility variation of all specimens.

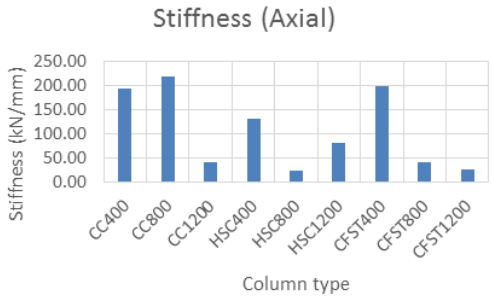

Fig. 17. Axial stiffness variation of all specimens.

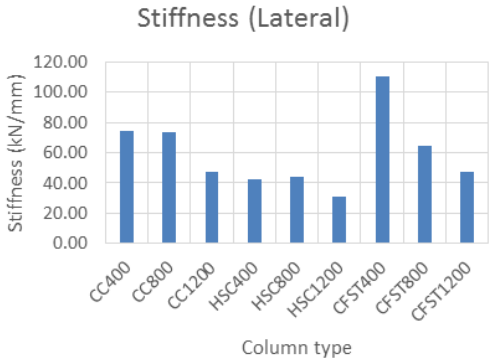

Fig. 18. Latertal stiffness variation of all specimens.

The axial stiffness of the concrete specimen was higher when its height was 800mm, while regarding the HSC and CFST specimens maximum axial stiffness was measured at 400mm. Maximum lateral stiffness of CC, HSC, and CFST was measured for specimen height of 400mm, 800mm, and 400mm respectively.

V. MODES OF FAILURE

The failure modes of all specimens are illustrated in Figure 19. The concrete specimens exhibited shear failure that caused cuts in plain concrete. The HSC specimens exhibited local buckling due to the end effect. The CFST specimens exhibited steel yielding and global buckling. When the applied load is increased, large axial strain is developed and the steel tubes fracture. In the CFST specimens, the presence of steel tubes provides confinement to the concrete core and worked as a composite that led to buckled failure mode.

Fig. 19. Failure modes of the tested specimens.

VI. DISCUSSION

Based on the experimental results, the strength capacity of each specimen is compared with the others of its group (Table VI) and with the other groups for specimens of the same height (Table VII). The smallest height within the same material gave the highest strength capacity because short specimens have low slenderness ratio. The CFST specimen gave higher strength than the others because they have higher stiffness due to the higher moment of inertia and equivalent modulus of elasticity due to the composite action between the concrete core and the surrounding steel tube. HSC exhibited the smallest strength carrying capacity because it has solid cross section.

TABLE VI. STRENGTH CARRYING CAPACITY WITHIN THE SAME MATERIAL

Mark	Height (mm)	Maximum load (kN)	% Decrease in load capacity
CC	400	224.00	---
	800	196.64	12.21
	1200	171.30	23.53
HSC	400	104.66	---
	800	99.40	5.03
	1200	96.08	8.20
CFST	400	415.08	---
	800	358.86	13.54
	1200	327.81	21.02

TABLE VII. STRENGTH CARRYING CAPACITY FOR SAME SPECIMEN HEIGHT

Height (mm)	Mark	Maximum load (kN)	% Increase in load capacity
400	HSC	104.66	---
	CC	224.00	114.03
	CFST	415.08	296.60
800	HSC	99.40	---
	CC	196.64	97.83
	CFST	358.86	261.03
1200	HSC	96.08	---
	CC	171.30	78.29
	CFST	327.81	281.18

Axial (longitudinal) displacement for long specimens (800 and 1200mm) increased as the height increased because axial displacement relies on the load and on the height (PL/AE), so for the same rigidity (AE) the displacement increased. Figure 3 shows that for the same load, the axial displacement developed in the HSC specimen was more than the other specimens' and the displacement of CFST was less. The same phenomena were observed and plotted for lateral displacement. Axial strain and lateral strain for CFST specimens were less than the other specimens' (CC and HSC) for the same reasons. The ductility of CFST specimens was more than the HSC and CC (brittle material-less ductility) specimens because the steel tubes surrounding the concrete core gave more strength without sudden failure and the displacement at failure load became more (large deformation). The stiffness of the CFST is more than the CC and HSC specimens' due to its capability of high strength capacity with low displacement. Also the composite action of CFST gave more stiffness (EI) due to its increased equivalent modulus of elasticity and transformed moment of inertia.

VII. CONCLUSION

The test results of the strength of composite columns under the effect of uniaxial compression loading, indicated that the shorter columns of the same material had higher strength capacity. The stiffness of composite specimens was higher than the concrete and hollow steel specimens'. The behavior and strength of composite column differed from steel and hollow steel due to the composite action between concrete and steel that gave higher strength and more realistic behavior. More study is required in order to investigate steel fiber concrete confined by steel tubes.

REFERENCES

[1] C. Wu, J. Li, and Y. Su, "5 - Ultra-high performance concrete-filled steel tubular columns," in *Development of Ultra-High Performance Concrete Against Blasts*, C. Wu, J. Li, and Y. Su, Eds. Woodhead Publishing, 2018, pp. 283–395.

[2] ACI Committee 440, *ACI PRC-440.2-17: Guide for the Design and Construction of Externally Bonded FRP Systems for Strengthening Concrete Structures*. ACI, 2017.

[3] M. H. Lai and J. C. M. Ho, "Confinement effect of ring-confined concrete-filled-steel-tube columns under uni-axial load," *Engineering Structures*, vol. 67, pp. 123–141, May 2014, https://doi.org/10.1016/j.engstruct.2014.02.013.

[4] L.-H. Han, W. Li, and R. Bjorhovde, "Developments and advanced applications of concrete-filled steel tubular (CFST) structures: Members," *Journal of Constructional Steel Research*, vol. 100, pp. 211–228, Sep. 2014, https://doi.org/10.1016/j.jcsr.2014.04.016.

[5] P. Li, T. Zhang, and C. Wang, "Behavior of Concrete-Filled Steel Tube Columns Subjected to Axial Compression," *Advances in Materials Science and Engineering*, vol. 2018, Aug. 2018, Art. no. e4059675, https://doi.org/10.1155/2018/4059675.

[6] J. Cai, J. Pan, and Q. Shan, "Failure mechanism of full-size concrete filled steel circle and square tubes under uniaxial compression," *Science China Technological Sciences*, vol. 58, no. 10, pp. 1638–1647, Oct. 2015, https://doi.org/10.1007/s11431-015-5890-4.

[7] A. K. H. Kwan, C. X. Dong, and J. C. M. Ho, "Axial and lateral stress–strain model for circular concrete-filled steel tubes with external steel confinement," *Engineering Structures*, vol. 117, pp. 528–541, Jun. 2016, https://doi.org/10.1016/j.engstruct.2016.03.026.

[8] L. He, S. Lin, and H. Jiang, "Confinement Effect of Concrete-Filled Steel Tube Columns With Infill Concrete of Different Strength Grades," *Frontiers in Materials*, vol. 6, 2019, https://doi.org/10.3389/fmats.2019.00071.

[9] F. Alatshan, S. A. Osman, R. Hamid, and F. Mashiri, "Stiffened concrete-filled steel tubes: A systematic review," *Thin-Walled Structures*, vol. 148, Mar. 2020, Art. no. 106590, https://doi.org/10.1016/j.tws.2019.106590.

[10] J.-Y. Zhu, J. Chen, and T.-M. Chan, "Analytical model for circular high strength concrete filled steel tubes under compression," *Engineering Structures*, vol. 244, Oct. 2021, Art. no. 112720, https://doi.org/10.1016/j.engstruct.2021.112720.

[11] T. Kibriya, "Performance of Concrete Filled Steel Tubular Columns," *American Journal of Civil Engineering and Architecture*, vol. 5, no. 2, pp. 35–39, 2017, https://doi.org/10.12691/ajcea-5-2-1.

[12] P. C. Nguyen, D. D. Pham, T. T. Tran, and T. Nghia-Nguyen, "Modified Numerical Modeling of Axially Loaded Concrete-Filled Steel Circular-Tube Columns," *Engineering, Technology & Applied Science Research*, vol. 11, no. 3, pp. 7094–7099, Jun. 2021, https://doi.org/10.48084/etasr.4157.

[13] L. Hamzaoui and T. Bouzid, "The Proposition of an EI Equation of Square and L–Shaped Slender Reinforced Concrete Columns under Combined Loading," *Engineering, Technology & Applied Science Research*, vol. 11, no. 3, pp. 7100–7106, Jun. 2021, https://doi.org/10.48084/etasr.4048.

[14] A. Ali, Z. Soomro, S. Iqbal, N. Bhatti, and A. F. Abro, "Prediction of Corner Columns' Load Capacity Using Composite Material Analogy," *Engineering, Technology & Applied Science Research*, vol. 8, no. 2, pp. 2745–2749, Apr. 2018, https://doi.org/10.48084/etasr.1879.

[15] *ASTM C39/C39M-15: Standard Test Method for Compressive Strength of Cylindrical Concrete Specimens*. ASTM, 2015.

[16] C09 Committee, "ASTM C496 / C496M - 11: Standard Test Method for Splitting Tensile Strength of Cylindrical Concrete Specimens," ASTM International. https://doi.org/10.1520/C0496_C0496M-11.

[17] *ASTM C293/C293M-16: Standard Test Method for Flexural Strength of Concrete (Using Simple Beam With Center-Point Loading)*. ASTM International, 2016.

[18] *ASTM C469/C469M-14: Standard Test Method for Static Modulus of Elasticity and Poisson's Ratio of Concrete in Compression Section 6 Instructional Video*. ASTM.

[19] *ASTM A370-21: Standard Test Methods and Definitions for Mechanical Testing of Steel Products*. ASTM.